RSC Advances

PAPER

View Article Online
View Journal | View Issue

Cite this: *RSC Adv.*, 2015, **5**, 93888

Low-viscosity ether-functionalized pyrazolium ionic liquids based on dicyanamide anions: properties and application as electrolytes for lithium metal batteries†

Shumin Shen,[a] Shaohua Fang,*[ac] Long Qu,[a] Dong Luo,[a] Li Yang*[abc] and Shin-ichi Hirano[b]

Received 29th August 2015
Accepted 27th October 2015

DOI: 10.1039/c5ra17539a

www.rsc.org/advances

Four new ether-functionalized pyrazolium ionic liquids (ILs) based on dicyanamide (DCA) anions are synthesized and characterized. The physical and electrochemical properties of these ILs, including melting point, thermal stability, viscosity, conductivity and electrochemical stability are investigated. All these ILs are liquids and their viscosities are lower than 40 mPa s at 25 °C. Though the four IL electrolytes with 0.6 mol kg^{-1} LiDCA have good chemical stability against lithium metals, only 1-(2-methoxyethyl)-2-methylpyrazolium dicyanamide (PZ2o1-1-DCA) and 1-(2-methoxyethyl)-2-ethylpyrazolium dicyanamide (PZ2o1-2-DCA) electrolytes can be used as electrolytes for lithium metal batteries due to the formation of a beneficial SEI film on the lithium metal during the cycling test of a symmetric lithium cell. At room temperature, Li/$LiFePO_4$ coin cells using the two electrolytes show good cycling performance at 0.1C, and the cell using PZ2o1-2-DCA electrolyte shows better rate performance.

1. Introduction

Ionic liquids (ILs) are low-temperature molten salts composed of organic cations and various anions, and they possess some attractive properties, such as low flammability, negligible volatility and high thermal stability.[1–4] Based on these properties, utilization of ILs as safe electrolytes for lithium ion/metal batteries has gained tremendous interest of researchers in the last decade.[5–10] However, ILs show high viscosity compared to conventional organic solvents, due to strong electrostatic force between cations and anions in ILs. In order to enhance the mobility of lithium ion in the IL electrolytes and the wettability of IL electrolytes to electrode and separator, considerable effort has been paid to reduce the viscosity of ILs by tuning the chemical structures of cation and anion.

Functionalization of cation is an effective approach to adjust the physicochemical properties of ILs, and it also provides more choices for applications of ILs.[11–15] Among different kinds of functional groups, one ether group with electron-donating action can contribute to the decrease of viscosity and melting point, and not result in the apparent deterioration of electrochemical and thermal stability.[16–20] Until now, one ether group has been incorporated into many types of IL cations, such as imidazolium,[16,21–23] tetraalkylammonium,[17,24] piperidinium,[18,25] pyrrolidinium[18] and tetraalkylphosphonium[19,26] cations. Owning to their superiority in viscosity and melting point, some ether-functionalized ILs have been selected as electrolytes for lithium metal batteries.[7,20,27–30]

Fluorinated sulfonyl type anions, such as bis(trifluoromethanesulfonyl)imide (TFSI) and bis(fluorosulfonyl)imide (FSI), can give ILs low-viscosity character owning to weakly coordinating nature and high charge delocalization.[25,31–40] Besides the advantage of viscosity, the ILs based on TFSI and FSI anions can possess high electrochemical stability and allow the reversible lithium redox on lithium metal, and they are often chosen as electrolytes in lithium metal batteries.[25,41–46] Nevertheless, the high cost of TFSI and FSI anions still restrict the practical applications of these ILs.

Another well-known anion to compose low-viscosity ILs is dicyanamide (DCA) anion with small size and high charge delocalization.[47,48] Since the pioneer work of MacFarlane *et al.* on bringing DCA anion into ILs, DCA-based imidazolium, tetraalkylammonium, pyrrolidinium, pyridinium, sulfonium, guanidinium and tetraalkylphosphonium ILs have been reported.[26,47–52] Considering the limited electrochemical stability of the DCA-based ILs, their electrochemical applications have

[a]*School of Chemistry and Chemical Engineering, Shanghai Jiao Tong University, Shanghai 200240, China. E-mail: housefang@sjtu.edu.cn; liyangce@sjtu.edu.cn; Fax: +86 21 54741297; Tel: +86 21 54748917*

[b]*Hirano Institute for Materials Innovation, Shanghai Jiao Tong University, Shanghai 200240, China*

[c]*Shanghai Electrochemical Energy Devices Research Center, Shanghai 200240, China*

† Electronic supplementary information (ESI) available. See DOI: 10.1039/c5ra17539a

been focused on dye-sensitized solar cell[53–56] and super capacitor.[57,58] Recently, Yoon *et al.* have proposed the DCA-based ILs as inexpensive non-fluorinated electrolytes for lithium metal batteries, and demonstrated the stable cycle performance of Li/$LiFePO_4$ coin cells using *N*-methyl-*N*-butylpyrrolidinium DCA (P14-DCA) and *N*-methyl-*N*-methylpyrrolidinium DCA (P11-DCA) electrolytes at high temperature.[10] This discovery greatly extends the potential applications of DCA-based ILs, and it also encourages the researchers to explore new DCA-based ILs as electrolytes for lithium metal batteries.

Pyrazolium cation has a structure of heteroaromatic ring analogous to imidazolium cation, but researches about pyrazolium ILs are rare in contrast to imidazolium ILs.[59–64] Several TFSI-based pyrazolium ILs have been proposed as electrolytes for lithium ion/metal batteries.[65–70] In this paper, we synthesized four new ILs composed of ether-functionalized pyrazolium cations and DCA anion, and the structures of these ILs were shown in Fig. 1. The physicochemical properties of these ILs were systematically studied. As expected, these ILs exhibited low-viscosity and high-conductivity characteristics. Chemical stability against lithium metal and cycle performance of symmetric lithium cells were investigated for these IL electrolytes with 0.6 mol kg^{-1} LiDCA, and charge–discharge characteristics of Li/$LiFePO_4$ cells were examined. It was demonstrated that PZ2o1-1-DCA and PZ2o1-2-DCA could be used as new DCA-based IL electrolytes for lithium metal batteries. Li/$LiFePO_4$ coin cells using the two electrolytes could exhibit stable cycling performance at 0.1C, and the cell using PZ2o1-2-DCA electrolyte showed better rate performance.

2. Experimental

2.1 Reagents and materials

Commercial reagents were purchased from Alfa Aesar or TCI Co., Ltd., and used as received. Lithium bis(trifluoromethanesulfonyl)imide (LiTFSI) was kindly provided by Morita Chemical Industries Co., Ltd. And lithium dicyanamide (LiDCA) was prepared according to the procedures described in the literatures.[10,71]

2.2 Synthesis of ether-functionalized pyrazolium ILs

Pyrazolium iodides were synthesized by alkylation of ether-functionalized pyrazoles with iodomethane or iodoethane, as the reported method.[68] And then anion exchange was carried out following the literatures.[18,48] Detailed procedures and NMR data of ^1H and ^{13}C were collected in the ESI.†

2.3 Measurement

^1H NMR and ^{13}C NMR spectra of ILs were measured by a Bruker spectrometer (Advance III HD 400). A Metrohm 73KF Karl Fischer coulometer was used to determine the water contents, and the water contents in these DCA-based ILs were lower than 100 ppm. Phase transition behavior of ILs was studied by a differential scanning calorimeter (DSC, TA Q2000). Each IL (about 5 mg) was sealed into a small aluminum crucible in dry atmosphere. After cooled from room temperature to −60 °C, the sample stayed at −60 °C for 15 minutes so as to insure complete crystallization (if possible), and then was heated from −60 °C to 60 °C. The above procedures were repeated twice at 10 °C min^{-1}. Thermal stability was detected by thermal gravimetric analysis (TA, Q5000 IQ). The sample was heated between room temperature and 600 °C in nitrogen atmosphere at the rate of 10 °C min^{-1}.

The measurement of density was performed by weighing each IL (1.00 mL) at 25 °C. Viscosity was determined by a Brookfield viscometer (DV-III), and conductivity was tested by a DDS-11A conductivity meter. The tests of viscosity and conductivity were carried out every 5 °C between 25 °C and 80 °C by a Brookfield temperature controller (TC-502). Electrochemical stability was analyzed by linear sweep voltammetry

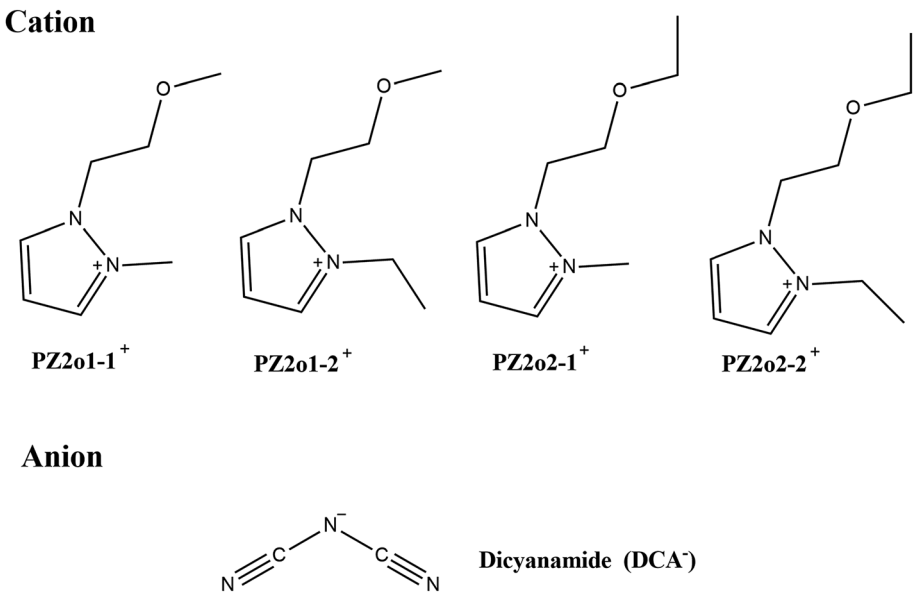

Fig. 1 Structure of these DCA-based ether-functionalized pyrazolium ILs.

(LSV) in an argon-filled glove box. Glassy carbon disk (3 mm diameter) was used as working electrode, and platinum wire and silver wire were chosen as counter and reference electrodes. Fresh IL was utilized for the positive and negative scans respectively. After each measurement, glassy carbon electrode should be polished with alumina paste.

0.6 mol kg^{-1} of LiDCA was dissolved in the dried IL in the glove box to obtain electrolyte. The water contents in PZ2o1-1-DCA, PZ2o1-2-DCA, PZ2o2-1-DCA and PZ2o2-2-DCA electrolytes were 98, 93, 96 and 91 ppm, respectively.

Symmetric lithium coin cell was fabricated in the glove box, and a PE separator (SK, 20 μm) was used. After the cell kept at open circuit for 2 days at room temperature, the cycling test was performed by a LAND test instrument (CT2001A). Current density was 0.1 mA cm^{-2}, and charge and discharge processes lasted for 16 min respectively.

Electrochemical performances of IL electrolytes for lithium metal battery were evaluated by coin cells. Cathode was composed of carbon coated $LiFePO_4$, acetylene black and PVDF (weight ratio 8 : 1 : 1), and coated onto aluminum foil (battery use). The loading of $LiFePO_4$ was around 2.0 mg cm^{-2}. Lithium foil was used as anode. After $LiFePO_4$ cathode was dried under vacuum at 110 °C, Li/$LiFePO_4$ coin cells using the PE separator (SK, 20 μm) were fabricated in the glove box. The cycling tests were conducted between 2.0 V and 4.0 V by a LAND test instrument. Current rate was determined basing on the theoretical capacity of $LiFePO_4$ (170 mA h g^{-1}).

The tests of LSV and electrochemical impedance spectrum (EIS) were conducted by a CHI660D electrochemistry workstation.

3. Results and discussion

3.1 Properties of ILs

Physicochemical properties of four DCA-based ether-functionalized pyrazolium ILs, such as melting point, thermal decomposition temperature, viscosity and conductivity, were summarized in Table 1.

All these ILs were liquid state at room temperature. Phase transition behavior was analyzed by differential scanning calorimeter (DSC), and the DSC curves of two ILs were illustrated in Fig. 2 as examples. PZ2o1-1-DCA exhibited a melting transition (T_m) after a crystallization transition (T_c). Like PZ2o1-2-DCA, three ILs did not display any phase transition behavior until −60 °C (the lower temperature limit of DSC measurement), and their melting points were defined as "<−60 °C" according to some published papers.[19,26,72] Generally, incorporating one ether group into different cations would be beneficial for decreasing the melting points of ILs, because of high flexibility of ether group, low symmetry of cation, and weak electrostatic attraction between cation and anion (caused by the electron-donating ability of ether group).[16–18] Hence, three new ether-functionalized pyrazolium ILs based on DCA anion could also possess the melting points lower than −60 °C, and they belonged to the low-melting point ILs. Moreover, it was found that PZ2o1-1-DCA showed the higher melting point (−8 °C) in these DCA-based pyrazolium ILs with the analogous structure of cation. As known, more flexible substituent in the cation could increase the conformational degrees of freedom, which would reduce the crystal lattice energy and help to realize the low melting points of ILs.[18] Considering that methyl group and 2-methoxyethyl group were less flexible than ethyl group and 2-ethoxyethyl group respectively, the lower conformational degrees of freedom of PZ2o1-1 cation mainly resulted in the higher melting point of PZ2o1-1-DCA.

The TGA curves of four ILs were presented in Fig. 3. PZ2o1-1-DCA and PZ2o2-1-DCA had the similar decomposition behavior, while the decomposition behavior of PZ2o1-2-DCA was approximate to that of PZ2o2-2-DCA. It was inferred that alkyl group at *N*-2 position of pyrazolium cation might affect the decomposition behavior. All the four ILs began to decompose at around 230 °C. The type of cation could make effect on the thermal stability of the DCA-based ILs. The thermal decomposition temperatures of the four pyrazolium ILs were close to those of tetraalkylammonium ILs, higher than those of sulfonium ILs (~180 °C), and lower than those of imidazolium (~270 °C), pyridinium (~250 °C) and pyrrolidinium (~250 °C)

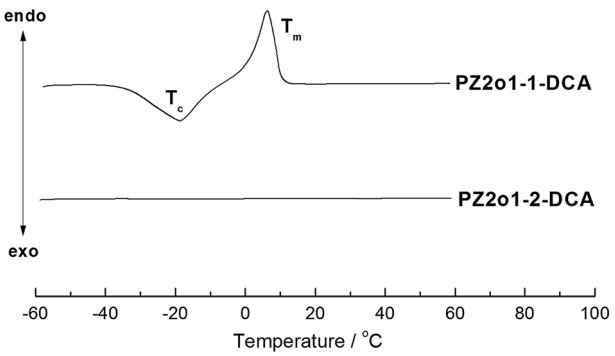

Fig. 2 DSC curves of PZ2o1-1-DCA and PZ2o1-2-DCA.

Table 1 Properties of these DCA-based ether-functionalized pyrazolium ILs

ILs	M_w[a]/g mol^{-1}	T_m[b]/°C	d[c]/g cm^{-3}	η[d]/mPa s	σ[e]/mS cm^{-1}	T_d[f]/°C
PZ2o1-1-DCA	207.24	−8	1.09	36.0	8.44	227.6
PZ2o1-2-DCA	221.26	<−60	1.08	33.6	8.27	227.8
PZ2o2-1-DCA	221.26	<−60	1.06	39.1	7.17	224.8
PZ2o2-2-DCA	235.29	<−60	1.04	32.4	7.79	227.0

[a] Molecular weight. [b] Melting point noted from the onset. [c] Density at 25 °C. [d] Viscosity at 25 °C. [e] Conductivity at 25 °C. [f] Decomposition temperature of 5% weight loss.

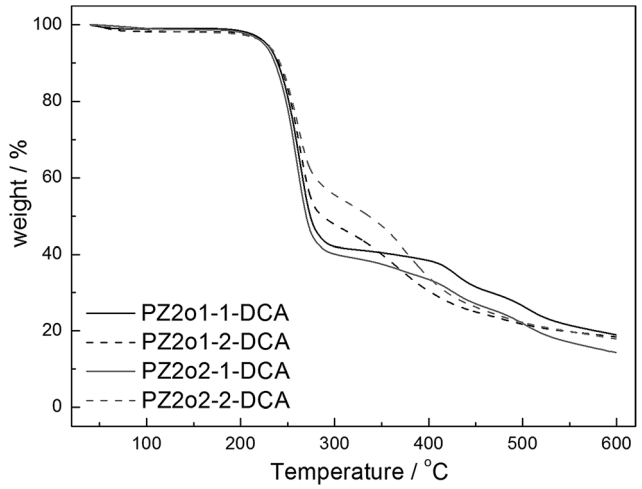

Fig. 3 TGA curves of these ILs.

ILs.[48–51] As known, the DCA-based ILs were not as thermally stable as the TFSI-based ILs.[48] Here, the four DCA-based pyrazolium ILs also showed lower thermal stability than the corresponding TFSI-based ILs (~340 °C).[69,70] However, compared to the conventional organic electrolytes containing highly volatile carbonates,[73] these DCA-based ILs still owned remarkable advantage in the thermal stability.

Table 2 Parameters of VTF equation for viscosity[a]

ILs	η_0 (mPa s)	B (K)	T_0 (K)	R^2
PZ2o1-1-DCA	0.17 ± 8%	588 ± 3%	189 ± 1%	0.99997
PZ2o1-2-DCA	0.15 ± 10%	633 ± 4%	182 ± 2%	0.99996
PZ2o2-1-DCA	0.17 ± 6%	615 ± 2%	185 ± 1%	0.99999
PZ2o2-2-DCA	0.16 ± 10%	626 ± 5%	181 ± 2%	0.99995

[a] The percentage standard errors for η_0, B and T_0 have been included, and R^2 is the VTF fitting parameter.

Table 3 Parameters of VTF equation for conductivity[a]

ILs	σ_0 (mS cm^{-1})	B (K)	T_0 (K)	R^2
PZ2o1-1-DCA	52 ± 11%	65 ± 19%	263 ± 2%	0.99391
PZ2o1-2-DCA	55 ± 10%	79 ± 17%	257 ± 2%	0.99615
PZ2o2-1-DCA	71 ± 12%	117 ± 16%	248 ± 2%	0.99736
PZ2o2-2-DCA	63 ± 11%	108 ± 16%	248 ± 2%	0.99738

[a] The percentage standard errors for σ_0, B and T_0 have been included, and R^2 is the VTF fitting parameter.

Viscosity of ILs was an important property for their chemical and electrochemical applications, and low viscosity was favorable for the mass transport in ILs. The viscosity of ILs could be mainly influenced by ion size, ion symmetry, and ion–ion interactions (including van der Waals interaction and electrostatic attraction).[74] The DCA-based imidazolium, tetraalkylammonium, pyrrolidinium, tetraalkylphosphonium and sulfonium ILs had lower viscosities than the corresponding TFSI-based ILs due to smaller size of DCA anion.[26,48,49] For the ether-functionalized pyrazolium ILs involved in this work, their viscosities were also reduced by substituting TFSI anion with

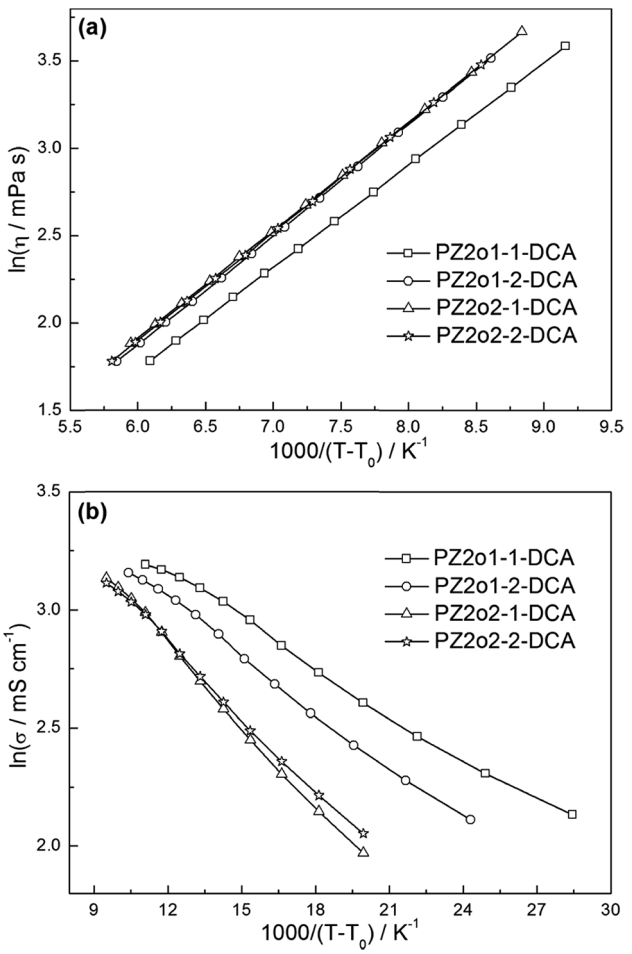

Fig. 4 VTF plots of (a) viscosity and (b) conductivity.

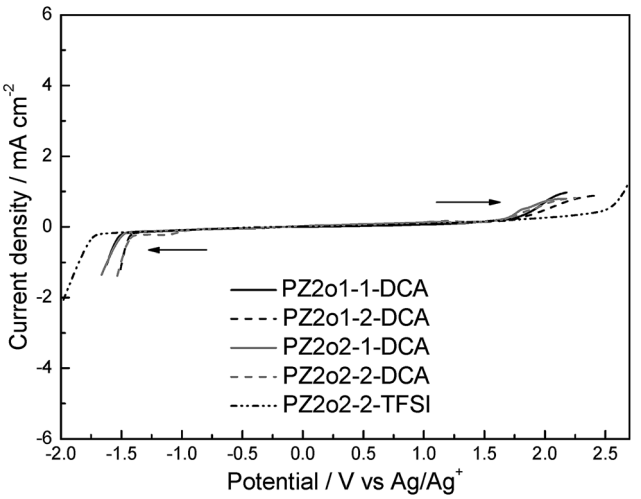

Fig. 5 LSV curves of these ILs at room temperature. Working electrode: glassy carbon; counter electrode: platinum wire; reference electrode: silver wire; scan rate: 10 mV s^{-1}.

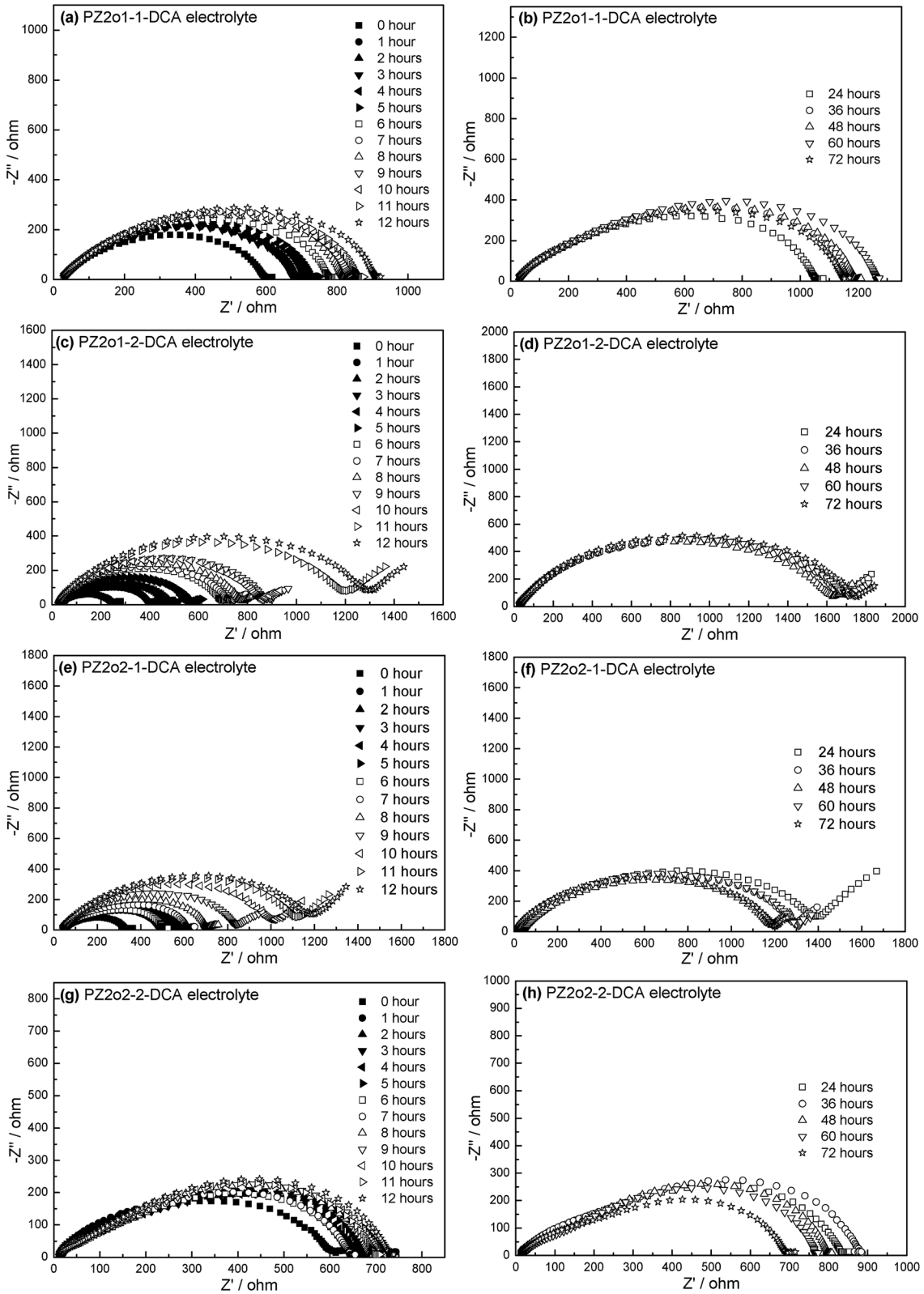

Fig. 6 Time evolution of impedance response for symmetric lithium cells under open circuit at room temperature: (a), (c), (e) and (g) from 0 to 12 hours; (b), (d), (f) and (h) from h to 72 hours.

DCA anion. For instance, the viscosity of PZ2o1-1-TFSI was 52.1 mPa s at 25 °C,[69] and the viscosity of PZ2o1-1-DCA was only 36.0 mPa s at 25 °C. According to Table 1, all the four DCA-based pyrazolium ILs had the viscosities lower than 40 mPa s at room temperature. Thus, they could be considered as a new series of low-viscosity ILs.

The changing of viscosity with temperature was studied between 25 °C and 80 °C for the four DCA-based ILs. As shown in Fig. 4a, the viscosity data were correlated by Vogel–Tammann–Fulcher (VTF) model according to eqn (1),

$$\eta = \eta_0 \exp\left(\frac{B}{T - T_0}\right) \quad (1)$$

where η_0 (mPa s), B (K) and T_0 (K) were adjustable parameters. The values of three parameters and the fitting coefficient R^2 were presented in Table 2. The temperature dependence of viscosity was in good agreement with VTF model in the temperature range studied. The η_0 and T_0 values of the four ILs were close to each other, and PZ2o1-1-DCA had the minimum B value. Compared to the corresponding TFSI-based pyrazolium ILs,[69,70] it was found that these DCA-based pyrazolium ILs had smaller B values and bigger T_0 values.

Usually, smaller sizes of cation and anion were favorable for increasing the conductivity of ILs. According to Table 1, PZ2o1-1-DCA had higher conductivity in the four ILs because of its smaller size of cation. Like other kinds of ILs,[26,49] these DCA-based pyrazolium ILs had obviously higher conductivities than the corresponding TFSI-based ILs. For example, the conductivity of PZ2o2-2-DCA (7.79 mS cm^{-1} at 25 °C) was more than two times higher than the conductivity of PZ2o2-2-TFSI (3.48 mS cm^{-1} at 25 °C).[70]

The conductivity as a function of temperature was investigated between 25 °C and 80 °C. As described in Fig. 4b, the conductivity data were also correlated by Vogel–Tammann–Fulcher (VTF) model according to eqn (2),

$$\sigma = \sigma_0 \exp\left(\frac{-B}{T - T_0}\right) \quad (2)$$

where σ_0 (mS cm^{-1}), B (K) and T_0 (K) were adjustable parameters. The values of three parameters and the fitting coefficient R^2 were summarized in Table 3. The temperature dependence of conductivity was also in agreement with VTF model. PZ2o2-1-DCA and PZ2o2-2-DCA had bigger σ_0 and B values and smaller T_0 values than PZ2o1-1-DCA and PZ2o1-2-DCA. Compared to the corresponding TFSI-based pyrazolium ILs,[69,70] the four DCA-based ILs owned smaller σ_0 and B values and bigger T_0 values.

The test results of LSV were used to identify the electrochemical stabilities of ILs. As illustrated in Fig. 5, the anodic limiting potentials of the four DCA-based pyrazolium ILs were around +1.8 V *versus* Ag/Ag$^+$. The cathodic limiting potentials of PZ2o1-1-DCA and PZ2o2-1-DCA were around −1.5 V *versus* Ag/Ag$^+$. For PZ2o1-2-DCA and PZ2o2-2-DCA, their cathodic limiting potentials were around −1.4 V *versus* Ag/Ag$^+$. So their electrochemical windows were about 3.2 V.

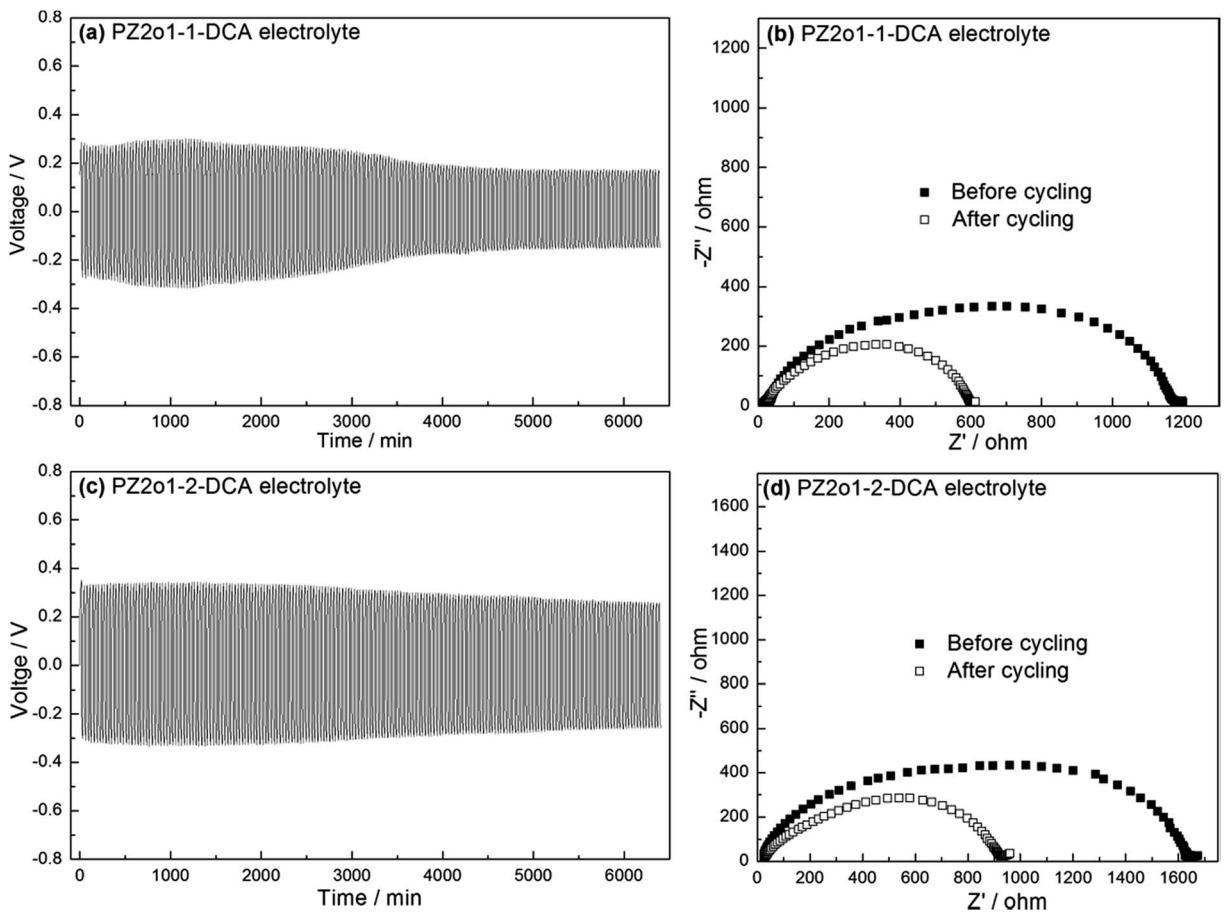

Fig. 7 Cycling and EIS results of symmetrical lithium cells: 0.1 mA cm^{-2} constant current and 200 cycles at room temperature: (a) and (b) PZ2o1-1-DCA electrolyte; (c) and (d) PZ2o1-2-DCA electrolyte.

Compared with the other kinds of DCA-based ILs, the electrochemical windows of these pyrazolium ILs were close to those of imidazolium ILs and narrower than those of tetraalkylammonium, tetraalkylphosphonium and pyrrolidinium ILs.[10,26,48] And the TFSI-based ether-functionalized pyrazolium ILs had wider electrochemical windows (about 4.4 V) than the DCA-based pyrazolium ILs in this work.[69,70] The LSV curves of one ether-functionalized pyrazolium IL with TFSI anion (PZ2o2-2-TFSI) were also presented as a reference. Apparently, the four DCA-based pyrazolium ILs exhibited lower anodic limiting potentials and higher cathodic limiting potentials than PZ2o2-2-TFSI. By referring to the electrochemical window of PZ2o2-2-TFSI *versus* Ag/Ag^+ (from −1.8 V to +2.6 V) and its electrochemical window *versus* Li/Li^+ (from +1.0 V to +5.4 V),[70] the cathodic and anodic limiting potentials *versus* Li/Li^+ of these DCA-based pyrazolium ILs were estimated to be about +1.4 V and +4.6 V respectively.

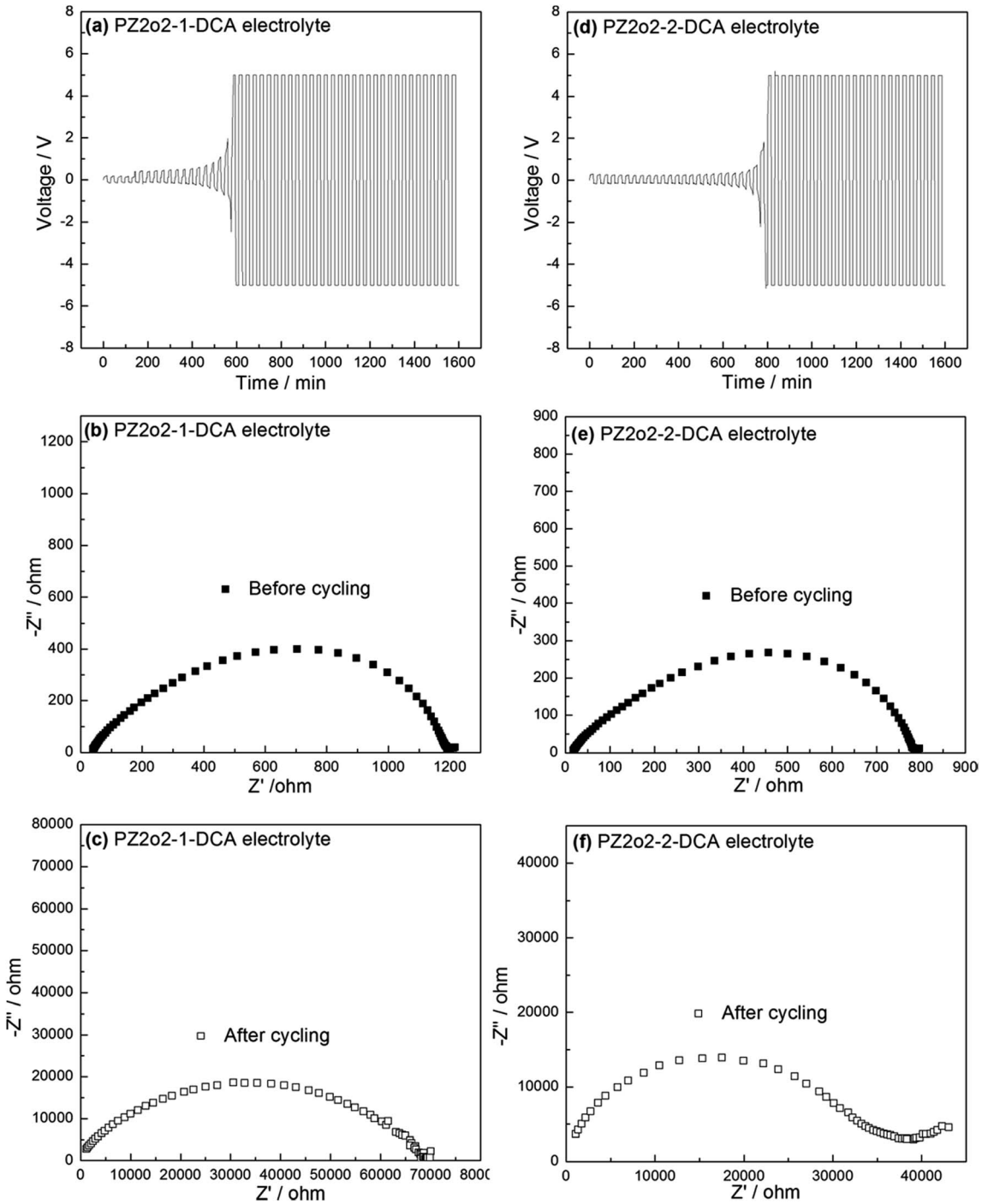

Fig. 8 Cycling and EIS results of symmetrical lithium cells: 0.1 mA cm^{-2} constant current and 50 cycles at room temperature: (a)–(c) PZ2o2-1-DCA electrolyte; (d)–(f) PZ2o2-2-DCA electrolyte.

3.2 Chemical stabilities of IL electrolytes against lithium metal

Fig. 6 showed the changing of EIS plots with time for symmetric lithium cells using four DCA-based IL electrolytes under open circuit at room temperature, and these results could help to determine the chemical stabilities and interfacial characteristics between electrolytes and lithium metal.[7,75–77] The intercept with real axis of EIS plot at high frequency was related to the bulk resistance of electrolyte, and the diameter of the semicircle represented the interfacial resistance (R_i) between electrolyte and lithium metal. For PZ2o1-1-DCA electrolyte (Fig. 6a and b), the R_i gradually increased from 0 to 12 hours, and after 48 hours the R_i value could keep dynamic stability. For the other three electrolytes, a similar phenomenon was observed. Considering that the cathodic limiting potentials of these DCA-based pyrazolium ILs were about +1.4 V *versus* Li/Li^+, the changing rule of R_i indicated that a passivation layer could form on lithium metal when IL electrolytes contacted with lithium metal, and the passivation layer would inhibit the reaction of IL electrolytes and lithium metal.

According to Fig. 6, when the R_i of these DCA-based pyrazolium IL electrolytes reached stability after 48 hours, the R_i values were in the range from 800 to 1600 Ω. These stable R_i values were bigger in comparison with the corresponding TFSI-based pyrazolium IL electrolytes.[69,70] For example, the R_i value of PZ2o1-2-DCA electrolyte was stable at about 1600 Ω, and PZ2o1-2-TFSI electrolyte showed a stable R_i value close to 500 Ω.[69] The water contents in these DCA-based IL electrolytes (90–100 ppm) were higher than those in the corresponding TFSI-based IL electrolytes (lower than 50 ppm).[69,70] Therefore, it was speculated that DCA anion and higher water content might result in the bigger interfacial resistance of DCA-based IL electrolyte/lithium metal.

3.3 Cycling performances of symmetric lithium cells

The symmetric lithium cells using the four DCA-based pyrazolium IL electrolytes were cycled at room temperature. Before the cycling tests, the cells had stayed under open circuit for 48 hours so that a stable passivation layer could form on lithium metal. The cycling results of PZ2o1-1-DCA and PZ2o1-2-DCA electrolytes and their EIS plots before and after cycling were shown in Fig. 7. For PZ2o1-1-DCA electrolyte, the voltage profile firstly increased and then decreased until it reached a steady state. For PZ2o1-2-DCA electrolyte, the voltage profile decreased gradually and then tended to stability. The diameter of the semicircle in the EIS plots was assigned to the interfacial

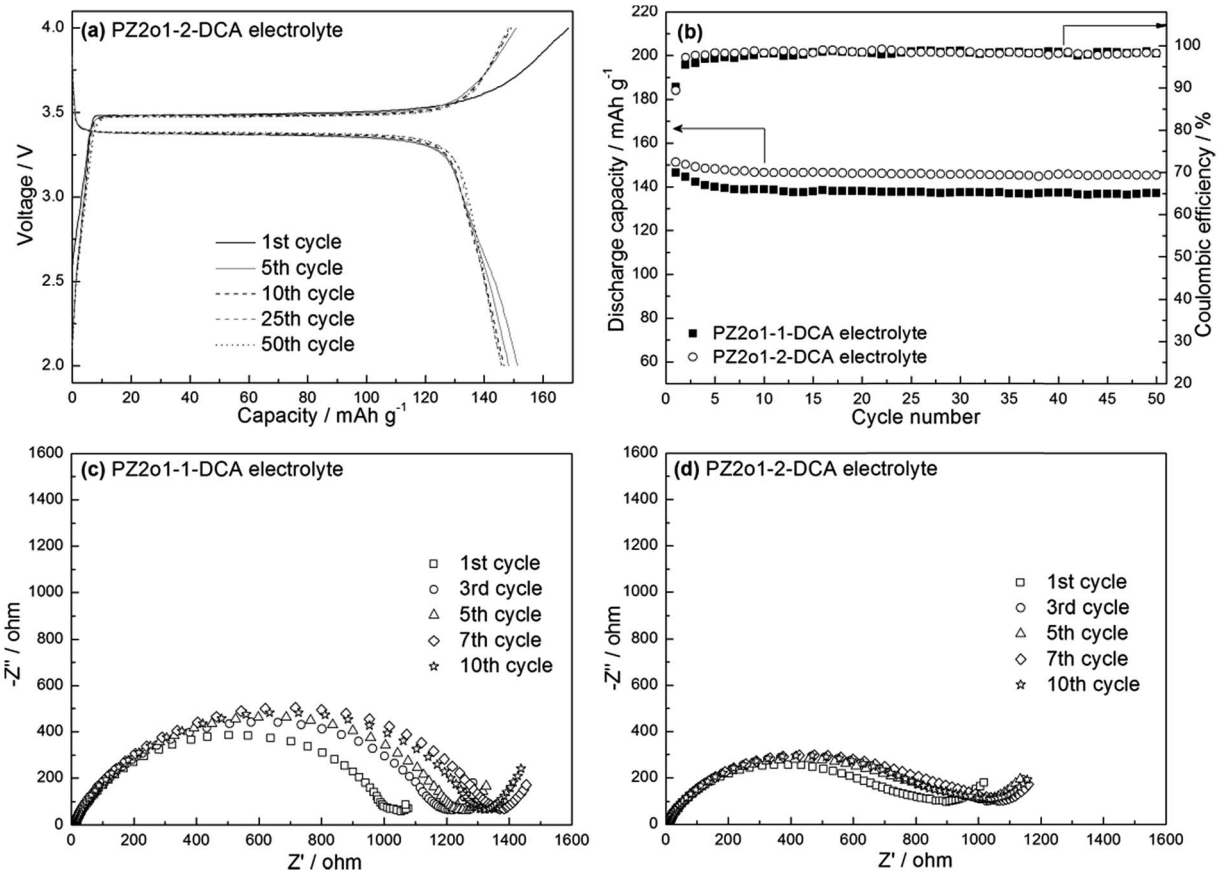

Fig. 9 (a) Charge–discharge curves of $Li/LiFePO_4$ cell using PZ2o1-2-DCA electrolyte, (b) discharge capacity and coulombic efficiency during cycling of $Li/LiFePO_4$ cells, and EIS plots of $Li/LiFePO_4$ cells using (c) PZ2o1-1-DCA and (d) PZ2o1-2-DCA electrolytes after different cycles at 0.1C at room temperature.

resistance of electrolyte/lithium metal. Apparently, the interfacial resistances of electrolyte/lithium metal became smaller after cycling test, which was consistent with the decreasing process of the voltage profile. And it also indicated that the initial passivation layer on lithium metal might turn into the solid electrolyte interphase (SEI) film during the cycling test. For PZ2o2-1-DCA and PZ2o2-2-DCA electrolytes, a different phenomenon could be observed. As illustrated in Fig. 8, the voltage profile increased quickly to 5 V, which was the voltage limit of the test instrument. And the interfacial resistances of electrolyte/lithium metal increased drastically after cycling test.

The previous report about P14-DCA electrolyte showed that the water content in electrolyte would affect the cycling performance of symmetric lithium cells and the SEI film on lithium metal at 50 °C.[10] Because the water contents in PZ2o2-1-DCA and PZ2o2-2-DCA electrolytes (96 and 91 ppm) were close to those of PZ2o1-1-DCA and PZ2o1-2-DCA electrolytes (98 and 93 ppm), their different electrochemical behavior of symmetric lithium cells could be attributed to the different ether groups in pyrazolium cations, which might affect the forming of SEI film on lithium metal. And the above results also manifested that PZ2o2-1-DCA and PZ2o2-2-DCA electrolytes were unsuitable as electrolytes for lithium metal batteries due to the worse interfacial characteristics of electrolyte/lithium metal.

3.4 Charge–discharge characteristics of Li/$LiFePO_4$ cells

In the innovative work of Yoon *et al.*,[10] the stable cycle performances of Li/$LiFePO_4$ cells using two DCA-based pyrrolidinium IL electrolytes (P14-DCA and P11-DCA electrolytes) could be obtained, when the cells were tested under the voltage range of 3.0–3.8 V at 50 or 80 °C. Regrettably, there was no performance comparison between the DCA-based IL electrolytes and the corresponding TFSI- or FSI-based IL electrolytes. In this work, the charge–discharge tests of Li/$LiFePO_4$ cells using PZ2o1-1-DCA and PZ2o1-2-DCA electrolytes were performed under the voltage range of 2.0–4.0 V, in order to compare with the previous results of Li/$LiFePO_4$ cells using PZ2o1-1-TFSI and PZ2o1-2-TFSI electrolytes.[69]

Fig. 9a showed the charge–discharge curves of Li/$LiFePO_4$ cell using PZ2o1-2-DCA electrolyte at 0.1C, and Fig. 9b illustrated the discharge capacity and coulombic efficiency during cycling of Li/$LiFePO_4$ cells at 0.1C at room temperature. The initial discharge capacities of PZ2o1-1-DCA and PZ2o1-2-DCA electrolytes were 147 and 151 mA h g^{-1} respectively. Their discharge capacities decreased in the first several cycles, and stabilized at about 138 and 146 mA h g^{-1} until the 50th cycle. The stable discharge capacity of PZ2o1-2-DCA electrolyte approximated those of PZ2o1-1-TFSI and PZ2o1-2-TFSI electrolytes (about 150 mA h g^{-1}) at 0.1C.[69] The coulombic efficiencies of the initial cycle for PZ2o1-1-DCA and PZ2o1-2-DCA electrolytes were 90% and 89% respectively, and the efficiencies became higher than 98% after several cycles. EIS was utilized to analyze how the interfacial property of electrode/electrolyte affected the electrochemical performance of Li/$LiFePO_4$ cells. The EIS plots of Li/$LiFePO_4$ cells after different cycles at 0.1C were presented in Fig. 9c and d. The diameter of the semicircle represented the interfacial resistance of SEI film. For PZ2o1-1-DCA and PZ2o1-2-DCA electrolytes, the interfacial resistance increased with cycle number and then kept steady. The trend was consistent with the decreasing of discharge capacity in the first several cycles. It was inferred that the increasing of interfacial resistance was caused by the gradual forming of stable SEI film. Additionally, the lower interfacial resistance of PZ2o1-2-DCA electrolyte just explained its higher discharge capacity at 0.1C compared to PZ2o1-1-DCA electrolyte.

Fig. 10a showed the rate dependence of discharge capacity for Li/$LiFePO_4$ cells at room temperature, and the discharge capacity was normalized in terms of the stable discharge capacity at 0.1C. It was easy to find that the discharge capacity deceased as the discharge rate increased. As shown in Fig. 10b, the discharge capacity of PZ2o1-2-DCA electrolyte at 0.5C was 130 mA h g^{-1}, which retained 89% of the capacity at 0.1C, and the discharge capacity at 1.5C was 97 mA h g^{-1}, which retained 66% of the capacity at 0.1C. Basing on the results of normalized capacity, the rate property of PZ2o1-2-DCA electrolyte was obviously better than that of PZ2o1-1-DCA electrolyte. And the rate property of PZ2o1-2-DCA electrolyte might benefit from its

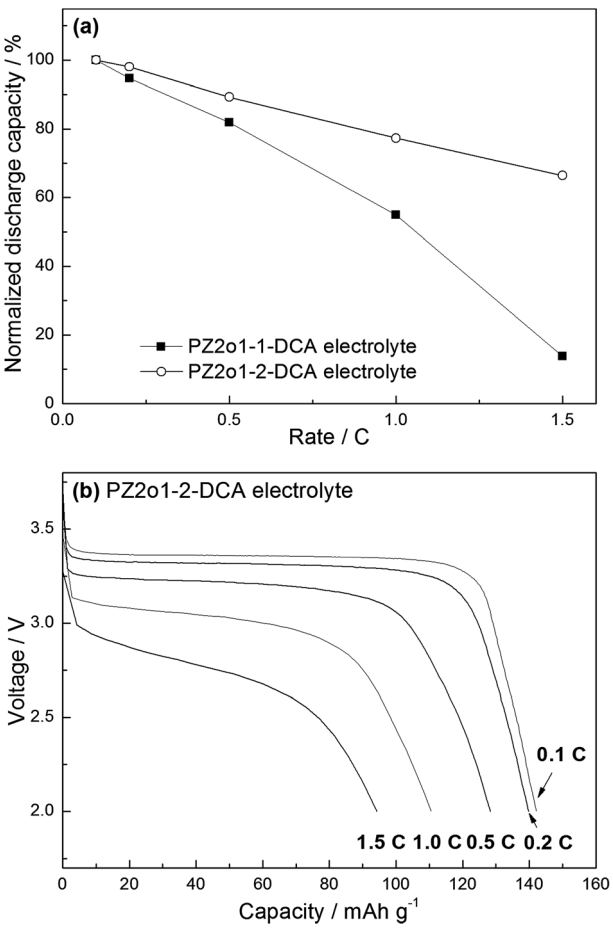

Fig. 10 (a) Rate dependence of normalized discharge capacity for Li/$LiFePO_4$ cells, and (b) the corresponding discharge curves of Li/$LiFePO_4$ cell using PZ2o1-2-DCA electrolyte at room temperature. Charge rate is 0.1C, and discharge rates are 0.1, 0.2, 0.5, 1.0 and 1.5C.

higher conductivity at room temperature (Table S1†) and lower interfacial resistance (as presented in Fig. 9c and d). Furthermore, although PZ2o1-1-DCA and PZ2o1-2-DCA had the advantages of viscosity and conductivity compared to PZ2o1-1-TFSI and PZ2o1-2-TFSI, the rate properties of PZ2o1-1-DCA and PZ2o1-2-DCA electrolytes were not as good as those of PZ2o1-1-TFSI and PZ2o1-2-TFSI electrolytes.[69] For example, the normalized capacity of PZ2o1-2-TFSI electrolyte at 1.0C was 81%,[69] and the normalized capacity of PZ2o1-2-DCA electrolyte at 1.0C was 77%. It also meant that the interfacial characteristics might be the major factor to affect the rate property of Li/$LiFePO_4$ cell. Therefore, the key point to improve the electrochemical performances of lithium metal batteries using the DCA-based IL electrolytes was how to optimize the interfacial characteristics by adjusting the structure of cations in DCA-based ILs.

The low-temperature performance of Li/$LiFePO_4$ cell at 0.1C was presented in Fig. 11a, and the discharge capacities at different temperatures were also normalized on the basis of the discharge capacity at 25 °C. Fig. 11b illustrated the discharge curves of PZ2o1-2-DCA electrolyte at different temperatures.

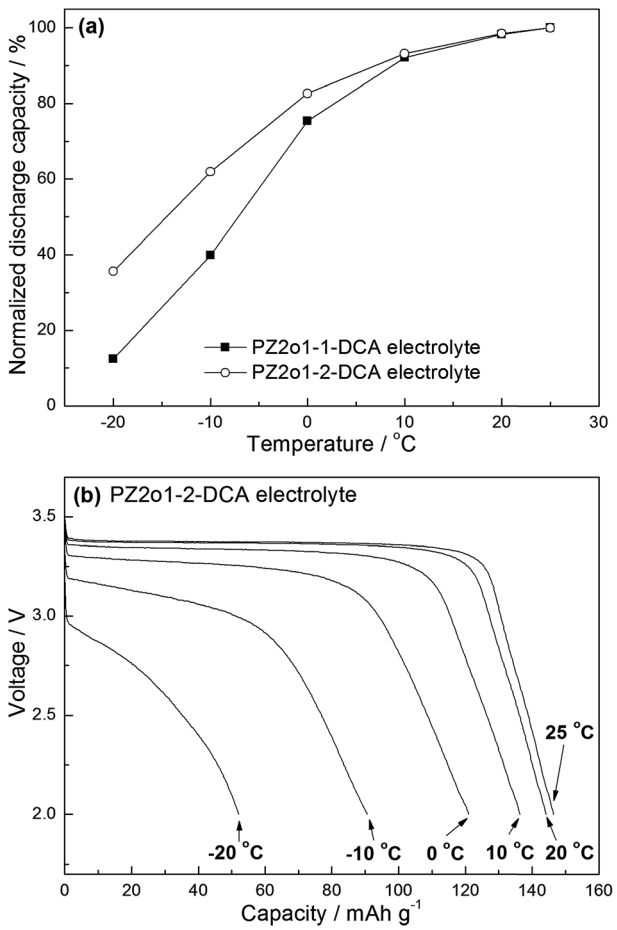

Fig. 11 (a) Temperature dependence of normalized discharge capacity for Li/$LiFePO_4$ cells at 0.1C, and (b) the corresponding discharge curves of Li/$LiFePO_4$ cell using PZ2o1-2-DCA electrolyte at different temperatures.

Obviously, the low-temperature performance of PZ2o1-2-DCA electrolyte was still better than that of PZ2o1-1-DCA electrolyte. For instance, the discharge capacity of PZ2o1-2-DCA electrolyte at −20 °C was 52 mA h g^{-1}, which retained 35.1% of the capacity at 25 °C, and the discharge capacity of PZ2o1-1-DCA electrolyte at −20 °C was only 17 mA h g^{-1}, which retained 12.4% of the capacity at 25 °C. According to the conductivities of PZ2o1-1-DCA and PZ2o1-2-DCA electrolytes between 25 °C and −20 °C (Table S1†), it could be found that PZ2o1-2-DCA electrolyte's advantage of conductivity became more prominent at low temperature. The conductivity of PZ2o1-2-DCA electrolyte was just 16% higher than that of PZ2o1-1-DCA electrolyte at 25 °C, while the conductivity of the former was 68% higher than the conductivity of the latter at −20 °C. Therefore, the significantly higher conductivity at low temperature was favorable to the low-temperature performance of PZ2o1-2-DCA electrolyte.

4. Conclusions

Four new ILs based on ether-functionalized pyrazolium cations and DCA anion were synthesized and characterized. The physicochemical properties of these ILs were systematically investigated. All the four ILs were liquids at room temperature, and three ILs showed melting points lower than −60 °C. The viscosities of the four ILs were lower than 40 mPa s, and their conductivities were higher than 7 mS cm^{-1} at 25 °C. The electrochemical windows of these ILs were about 3.2 V. Though the cathodic limiting potentials of these ILs was far higher than 0 V *versus* Li/Li^+, their IL electrolytes with 0.6 mol kg^{-1} LiDCA had good chemical stability against lithium metal owing to the forming of passivation layer. For PZ2o1-1-DCA and PZ2o1-2-DCA electrolytes, the cycling test results of symmetric lithium cells indicated that a stable SEI film could be formed on lithium metal after 200 cycles. At room temperature, Li/$LiFePO_4$ cells using PZ2o1-1-DCA and PZ2o1-2-DCA electrolytes showed good cycling performance at 0.1C, and the cell using PZ2o1-2-DCA electrolyte owned better rate performance.

Acknowledgements

This work is financially supported by the National Natural Science Foundation of China (Grants No. 21173148 and 21373136).

References

1 T. Welton, *Chem. Rev.*, 1999, **99**, 2071–2083.
2 J. Dupont, R. F. de Souza and P. A. Z. Suarez, *Chem. Rev.*, 2002, **102**, 3667–3692.
3 M. Armand, F. Endres, D. R. MacFarlane, H. Ohno and B. Scrosati, *Nat. Mater.*, 2009, **8**, 621–629.
4 D. R. Macfarlane, N. Tachikawa, M. Forsyth, J. M. Pringle, P. C. Howlett, G. D. Elliott, J. H. Davis, M. Watanabe, P. Simon and C. A. Angell, *Energy Environ. Sci.*, 2014, **7**, 232–250.
5 H. Sakaebe and H. Matsumoto, *Electrochem. Commun.*, 2003, **5**, 594–598.

6 M. Egashira, H. Todo, N. Yoshimoto, M. Morita and J. I. Yamaki, *J. Power Sources*, 2007, **174**, 560–564.
7 S. Seki, Y. Ohno, H. Miyashiro, Y. Kobayashi, A. Usami, Y. Mita, N. Terada, K. Hayamizu, S. Tsuzuki and M. Watanabe, *J. Electrochem. Soc.*, 2008, **155**, A421–A427.
8 K. Tsunashima, F. Yonekawa and M. Sugiya, *Chem. Lett.*, 2008, **37**, 314–315.
9 S. Fang, L. Yang, J. Wang, H. Q. Zhang, K. Tachibana and K. Kamijima, *J. Power Sources*, 2009, **191**, 619–622.
10 H. Yoon, G. H. Lane, Y. Shekibi, P. C. Howlett, M. Forsyth, A. S. Best and D. R. MacFarlane, *Energy Environ. Sci.*, 2013, **6**, 979–986.
11 J. H. Davis Jr, *Chem. Lett.*, 2004, **33**, 1072–1077.
12 Z. Fei, T. J. Geldbach, D. Zhao and P. J. Dyson, *Chem.–Eur. J.*, 2006, **12**, 2122–2130.
13 A. D. Sawant, D. G. Raut, N. B. Darvatkar, U. V. Desai and M. M. Salunkhe, *Catal. Commun.*, 2010, **12**, 273–276.
14 Y. Zhang, H. Gao, Y. H. Joo and J. M. Shreeve, *Angew. Chem., Int. Ed.*, 2011, **50**, 9554–9562.
15 D. M. Drab, M. Smiglak, J. L. Shamshina, S. P. Kelley, S. Schneider, T. W. Hawkins and R. D. Rogers, *New J. Chem.*, 2011, **35**, 1701–1717.
16 Z. B. Zhou, H. Matsumoto and K. Tatsumi, *Chem.–Eur. J.*, 2004, **10**, 6581–6591.
17 Z. B. Zhou, H. Matsumoto and K. Tatsumi, *Chem.–Eur. J.*, 2005, **11**, 752–766.
18 Z. B. Zhou, H. Matsumoto and K. Tatsumi, *Chem.–Eur. J.*, 2006, **12**, 2196–2212.
19 K. Tsunashima and M. Sugiya, *Electrochem. Commun.*, 2007, **9**, 2353–2358.
20 S. Fang, Y. Tang, X. Tai, L. Yang, K. Tachibana and K. Kamijima, *J. Power Sources*, 2011, **196**, 1433–1441.
21 Z. Fei, W. H. Ang, D. Zhao, R. Scopelliti, E. E. Zvereva, S. A. Katsyuba and P. J. Dyson, *J. Phys. Chem. B*, 2007, **111**, 10095–10108.
22 W. A. Henderson, V. G. Young Jr, D. M. Fox, H. C. de Long and P. C. Trulove, *Chem. Commun.*, 2006, 3708–3710.
23 Q. Liu, M. H. A. Janssen, F. van Rantwijk and R. A. Sheldon, *Green Chem.*, 2005, **7**, 39–42.
24 H. Matsumoto, M. Yanagida, K. Tanimoto, M. Nomura, Y. Kitagawa and Y. Miyazaki, *Chem. Lett.*, 2000, 922–923.
25 H. Matsumoto, H. Sakaebe and K. Tatsumi, *J. Power Sources*, 2005, **146**, 45–50.
26 K. Tsunashima, S. Kodama, M. Sugiya and Y. Kunugi, *Electrochim. Acta*, 2010, **56**, 762–766.
27 S. Seki, Y. Kobayashi, H. Miyashiro, Y. Ohno, Y. Mita, A. Usami, N. Terada and M. Watanabe, *Electrochem. Solid-State Lett.*, 2005, **8**, A577–A578.
28 K. Tsunashima, F. Yonekawa and M. Sugiya, *Electrochem. Solid-State Lett.*, 2009, **12**, A54–A57.
29 T. Sato, T. Maruo, S. Marukane and K. Takagi, *J. Power Sources*, 2004, **138**, 253–261.
30 S. Ferrari, E. Quartarone, P. Mustarelli, A. Magistris, M. Fagnoni, S. Protti, C. Gerbaldi and A. Spinella, *J. Power Sources*, 2010, **195**, 559–566.
31 P. Johansson, S. P. Gejji, J. Tegenfeldt and J. Lindgren, *Electrochim. Acta*, 1998, **43**, 1375–1379.
32 D. R. McFarlane, J. Sun, J. Golding, P. Meakin and M. Forsyth, *Electrochim. Acta*, 2000, **45**, 1271–1278.
33 H. Matsumoto, H. Kageyama and Y. Miyazaki, *Chem. Commun.*, 2002, 1726–1727.
34 H. Xue, R. Verma and J. M. Shreeve, *J. Fluorine Chem.*, 2006, **127**, 159–176.
35 H. B. Han, K. Liu, S. W. Feng, S. S. Zhou, W. F. Feng, J. Nie, H. Li, X. J. Huang, H. Matsumoto, M. Armand and Z. B. Zhou, *Electrochim. Acta*, 2010, **55**, 7134–7144.
36 H. B. Han, J. Nie, K. Liu, W. K. Li, W. F. Feng, M. Armand, H. Matsumoto and Z. B. Zhou, *Electrochim. Acta*, 2010, **55**, 1221–1226.
37 J. Reiter, S. Jeremias, E. Paillard, M. Winter and S. Passerini, *Phys. Chem. Chem. Phys.*, 2013, **15**, 2565–2571.
38 G. A. Giffin, N. Laszczynski, S. Jeong, S. Jeremias and S. Passerini, *J. Phys. Chem. C*, 2013, **117**, 24206–24212.
39 J. Reiter, E. Paillard, L. Grande, M. Winter and S. Passerini, *Electrochim. Acta*, 2013, **91**, 101–107.
40 P. Meister, V. Siozios, J. Reiter, S. Klamor, S. Rothermel, O. Fromm, H. W. Meyer, M. Winter and T. Placke, *Electrochim. Acta*, 2014, **130**, 625–633.
41 K. Tsunashima, A. Kawabata, M. Matsumiya, S. Kodama, R. Enomoto, M. Sugiya and Y. Kunugi, *Electrochem. Commun.*, 2011, **13**, 178–181.
42 H. Matsumoto, H. Sakaebe, K. Tatsumi, M. Kikuta, E. Ishiko and M. Kono, *J. Power Sources*, 2006, **160**, 1308–1313.
43 A. S. Best, A. I. Bhatt and A. F. Hollenkamp, *J. Electrochem. Soc.*, 2010, **157**, A903–A911.
44 A. I. Bhatt, A. S. Best, J. Huang and A. F. Hollenkamp, *J. Electrochem. Soc.*, 2010, **157**, A66–A74.
45 G. H. Lane, A. S. Best, D. R. MacFarlane, A. F. Hollenkamp and M. Forsyth, *J. Electrochem. Soc.*, 2010, **157**, A876–A884.
46 A. Basile, A. F. Hollenkamp, A. I. Bhatt and A. P. O'Mullane, *Electrochem. Commun.*, 2013, **27**, 69–72.
47 D. R. MacFarlane, J. Golding, S. Forsyth, M. Forsyth and G. B. Deacon, *Chem. Commun.*, 2001, 1430–1431.
48 D. R. MacFarlane, S. A. Forsyth, J. Golding and G. B. Deacon, *Green Chem.*, 2002, **4**, 444–448.
49 D. Gerhard, S. C. Alpaslan, H. J. Gores, M. Uerdingen and P. Wasserscheid, *Chem. Commun.*, 2005, 5080–5082.
50 P. S. Kulkarni, L. C. Branco, J. G. Crespo, M. C. Nunes, A. Raymundo and C. A. M. Afonso, *Chem.–Eur. J.*, 2007, **13**, 8478–8488.
51 N. Papaiconomou, J. Estager, Y. Traore, P. Bauduin, C. Bas, S. Legeai, S. Viboud and M. Draye, *J. Chem. Eng. Data*, 2010, **55**, 1971–1979.
52 C. M. S. S. Neves, K. A. Kurnia, J. A. P. Coutinho, I. M. Marrucho, J. N. C. Lopes, M. G. Freire and L. P. N. Rebelo, *J. Phys. Chem. B*, 2013, **117**, 10271–10283.
53 P. Wang, S. M. Zakeeruddin, J. E. Moser and M. Grätzel, *J. Phys. Chem. B*, 2003, **107**, 13280–13285.
54 R. Kawano, H. Matsui, C. Matsuyama, A. Sato, M. A. B. H. Susan, N. Tanabe and M. Watanabe, *J. Photochem. Photobiol., A*, 2004, **164**, 87–92.
55 Q. Dai, D. B. Menzies, D. R. MacFarlane, S. R. Batten, S. Forsyth, L. Spiccia, Y. B. Cheng and M. Forsyth, *C. R. Chim.*, 2006, **9**, 617–621.

56 C. Ning, Z. Jing, Z. Difei, Y. Zhihui, G. Jin and W. Peng, *J. Phys. Chem. C*, 2009, **113**, 4215–4221.
57 E. Frackowiak, G. Lota and J. Pernak, *Appl. Phys. Lett.*, 2005, **86**, 1–3.
58 F. B. Sillars, S. I. Fletcher, M. Mirzaeian and P. J. Hall, *Phys. Chem. Chem. Phys.*, 2012, **14**, 6094–6100.
59 Y. Abu-Lebdeh, P. J. Alarco and M. Armand, *Angew. Chem., Int. Ed.*, 2003, **42**, 4499–4501.
60 P. J. Alarco, Y. Abu-Lebdeh and M. Armand, *Solid State Ionics*, 2004, **175**, 717–720.
61 N. Ishimaru, W. Kubo, T. Kitamura, S. Yanagida, Y. Tsukahara, M. M. Maitani and Y. Wada, *Mater. Sci. Eng., B*, 2011, **176**, 996–1001.
62 N. A. Negm, M. M. Said and S. M. I. Morsy, *J. Surfactants Deterg.*, 2010, **13**, 521–528.
63 Y. Han, H. V. Huynh and G. K. Tan, *Organometallics*, 2007, **26**, 6581–6585.
64 C. Chiappe, A. Sanzone, D. Mendola, F. Castiglione, A. Famulari, G. Raos and A. Mele, *J. Phys. Chem. B*, 2013, **117**, 668–676.
65 P. J. Alarco, Y. Abu-Lebdeh, N. Ravet and M. Armand, *Solid State Ionics*, 2004, **172**, 53–56.
66 Y. Abu-Lebdeh, A. Abouimrane, P. J. Alarco and M. Armand, *J. Power Sources*, 2006, **154**, 255–261.
67 S. Seki, T. Kobayashi, N. Serizawa, Y. Kobayashi, K. Takei, H. Miyashiro, K. Hayamizu, S. Tsuzuki, T. Mitsugi, Y. Umebayashi and M. Watanabe, *J. Power Sources*, 2010, **195**, 6207–6211.
68 M. Chai, Y. Jin, S. Fang, L. Yang, S. I. Hirano and K. Tachibana, *Electrochim. Acta*, 2012, **66**, 67–74.
69 M. Chai, Y. Jin, S. Fang, L. Yang, S. I. Hirano and K. Tachibana, *J. Power Sources*, 2012, **216**, 323–329.
70 J. Zhang, S. Fang, L. Qu, Y. Jin, L. Yang and S. I. Hirano, *J. Appl. Electrochem.*, 2015, **45**, 235–244.
71 A. P. Purdy, E. Houser and C. F. George, *Polyhedron*, 1997, **16**, 3671–3679.
72 M. Kärnä, M. Lahtinen and J. Valkonen, *J. Mol. Struct.*, 2009, **922**, 64–76.
73 N. Wongittharom, T. C. Lee, I. M. Hung, S. W. Lee, Y. C. Wang and J. K. Chang, *J. Mater. Chem. A*, 2014, **2**, 3613–3620.
74 P. Bonĥte, A. P. Dias, N. Papageorgiou, K. Kalyanasundaram and M. Grätzel, *Inorg. Chem.*, 1996, **35**, 1168–1178.
75 S. Seki, Y. Ohno, Y. Kobayashi, H. Miyashiro, A. Usami, Y. Mita, H. Tokuda, M. Watanabe, K. Hayamizu, S. Tsuzuki, M. Hattori and N. Terada, *J. Electrochem. Soc.*, 2007, **154**, A173–A177.
76 A. Fernicola, F. Croce, B. Scrosati, T. Watanabe and H. Ohno, *J. Power Sources*, 2007, **174**, 342–348.
77 S. Ferrari, E. Quartarone, P. Mustarelli, A. Magistris, S. Protti, S. Lazzaroni, M. Fagnoni and A. Albini, *J. Power Sources*, 2009, **194**, 45–50.